# Supporting Information

## Confinement of iodine molecules into triple-helical chains within robust metal–organic frameworks

Xinran Zhang,[1] Ivan da Silva,[2] Harry G.W. Godfrey,[1] Samantha K. Callear,[2] Sergey A. Sapchenko,[1,3] Yongqiang Cheng,[4] Inigo Vitórica-Yrezábal,[1] Mark D. Frogley,[5] Gianfelice Cinque,[5] Chiu C. Tang,[5] Carlotta Giacobbe,[6] Catherine Dejoie,[6] Svemir Rudić,[2] Anibal J. Ramirez-Cuesta,[4] Melissa A. Denecke[1], Sihai Yang[1]* and Martin Schröder[1]*

[[1]] School of Chemistry, University of Manchester, Manchester, M13 9PL (UK)
E-mail: Sihai.Yang@manchester.ac.uk; M.Schroder@manchester.ac.uk

[[2]] ISIS Facility, STFC Rutherford Appleton Laboratory, Chilton, Oxfordshire, OX11 0QX (UK)

[[3]] Nikolaev Institute of Inorganic Chemistry, Siberian Branch of the Russian Academy of Sciences, Novosibirsk, 630090 (Russia)

[[4]] The Chemical and Engineering Materials Division (CEMD), Neutron Sciences Directorate, Oak Ridge National Laboratory, Oak Ridge, TN 37831 (USA)

[[5]] Diamond Light Source, Harwell Science Campus, Oxfordshire, OX11 0DE (UK)

[[6]] European Synchrotron Radiation Facility, Grenoble, 38043 (France)

## 1. Experiments and methods

All materials were purchased from commercially available sources, and used without further purification. Iodine (99.8% ACS) was purchased from Sigma-Aldrich.

### 1.1 Synthesis of MFM-300 materials

1.1.1 Synthesis of MFM-300(Al)

Biphenyl-3,3',5,5'-tetracarboxylic acid ($H_4L$, 60 mg, 0.182 mmol) and $Al(NO_3)_3{\cdot}9H_2O$ (340mg, 0.906 mmol) were added to a mixture of water (9 mL), piperazine (3 mL) and 2.8M $HNO_3$ (2 mL). The solution was heated in a 24 mL bomb at 483K for 3 days. The tan product was separated by filtration, washed with water and DMF several times and dried in air.

1.1.2 Synthesis of MFM-300(In)

Biphenyl-3,3',5,5'-tetracarboxylic acid ($H_4L$, 330 mg, 1 mmol) and $In(NO_3)_3.3H_2O$ (585 mg, 1.65 mmol) were added to a mixture of DMF (20 mL), MeCN (10 mL) and 70% nitric acid (1 mL). The solution was heated in a pressure flask at 363K for 3 days. The white product was separated by filtration, washed with DMF several times and dried in air.

1.1.3 MFM-300(Sc)

Biphenyl-3,3',5,5'-tetracarboxylic acid ($H_4L$, 300 mg, 0.91 mmol) and scandium triflate (900 mg, 1.83 mmol) were mixed in DMF (105 mL), water (15 mL) and HCl (36.5%, 3 mL). The solution was placed in a round bottom pressure flask and heated in an oil bath to $80^o$ for 72h. The white product was separated by filtration, washed with DMF and dried in air.

### 1.2 In-house powder X-ray diffraction analysis

Powder X-Ray Diffraction (PXRD) data were collected in flat plate mode over the 2θ range 5-40° on a X'pert multipurpose Diffractometer using Cu-Kα radiation (λ = 1.54056 Å) at 40 kV and 30 mA.

### 1.3 SEM experiments

SEM measurements were undertaken on a Zeiss EVO60 at a working voltage of 20kv with a scale bar up to 2 microns. The EDX experiment was undertaken using an EDS7636 SiLi dectector.

## 2. Additional Results

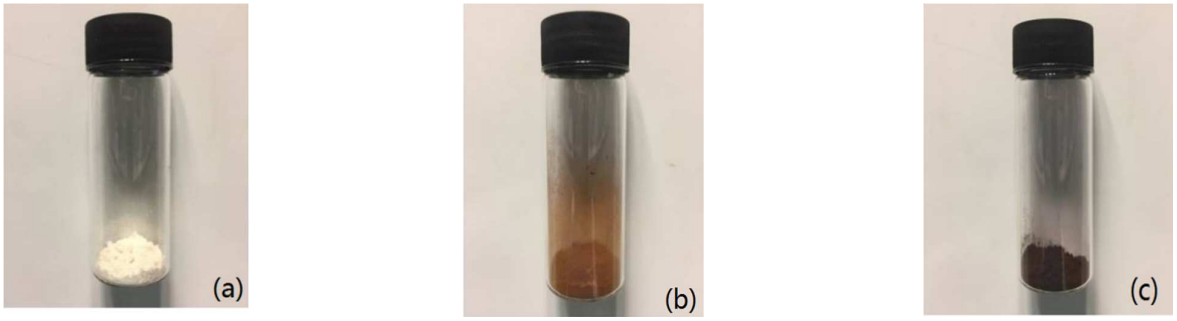


Figure S1: Views of samples: (a) MFM-300(Sc), (b) MFM-300(Sc)·1.11$I_2$ and (c) MFM-300(Sc)·2.62$I_2$.

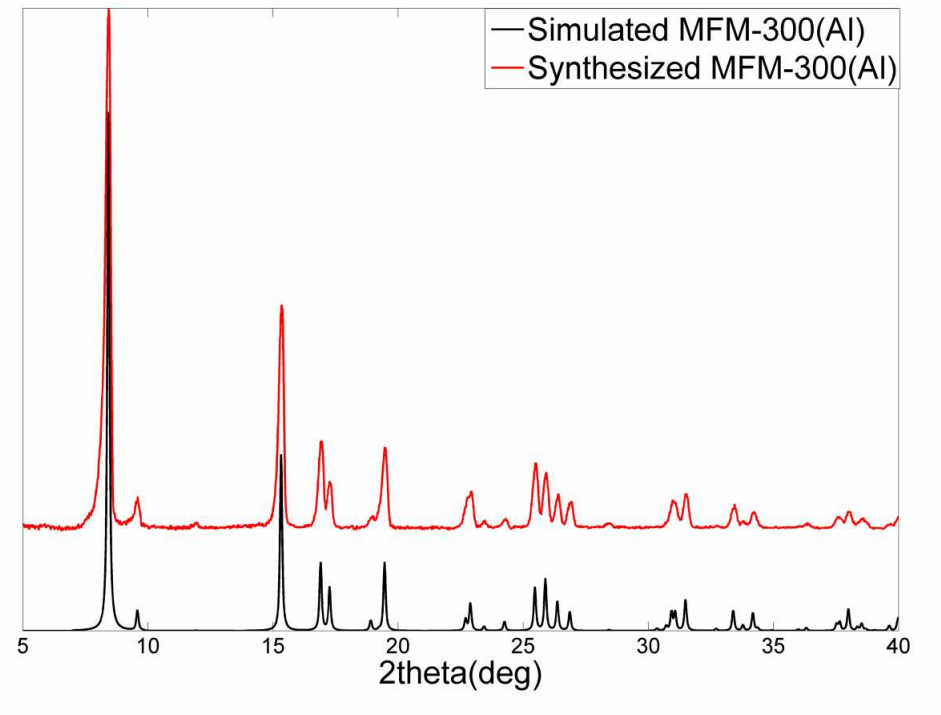


Figure S2: PXRD patterns for solvated MFM-300(Al)

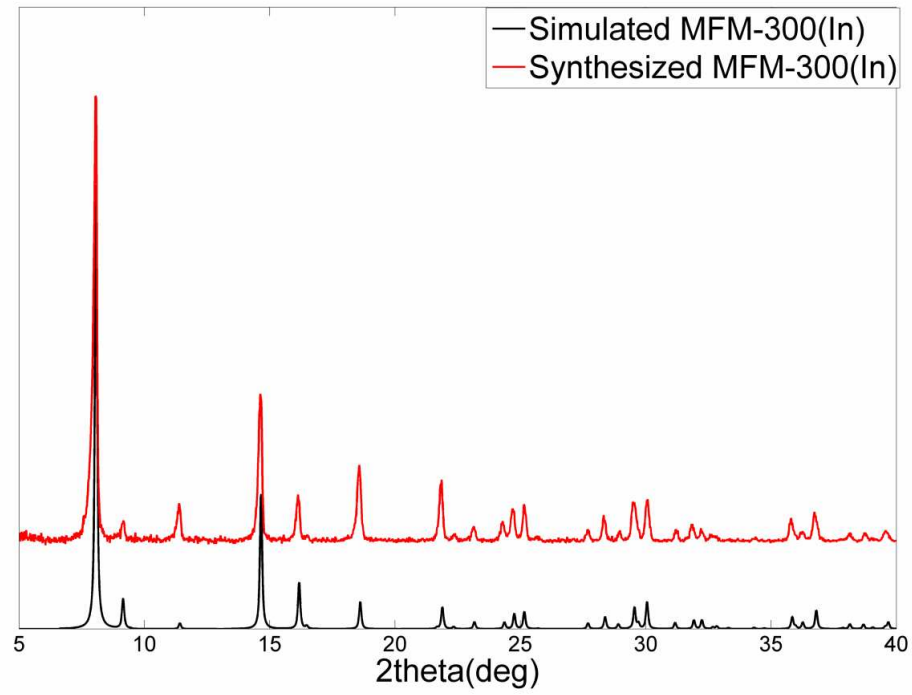


Figure S3: PXRD patterns for solvated MFM-300(In).

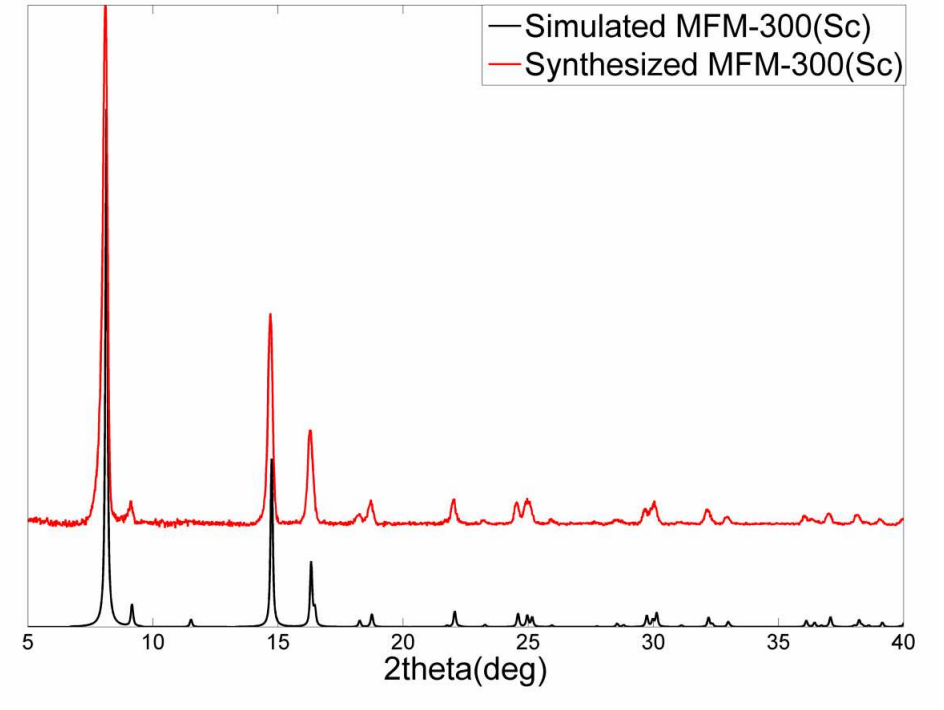


Figure S4: PXRD patterns for solvated MFM-300(Sc).

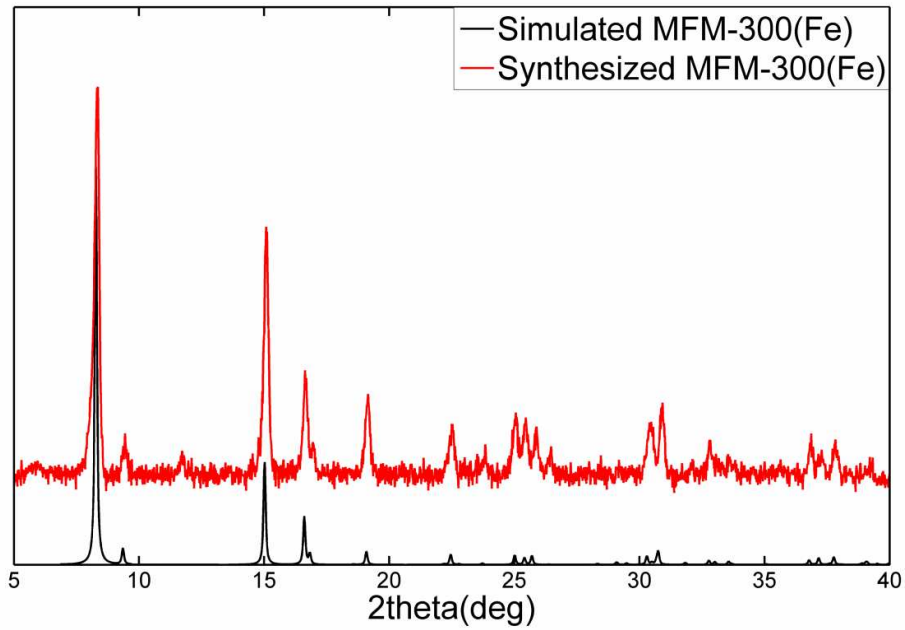


Figure S5: PXRD patterns for solvated MFM-300(Fe).

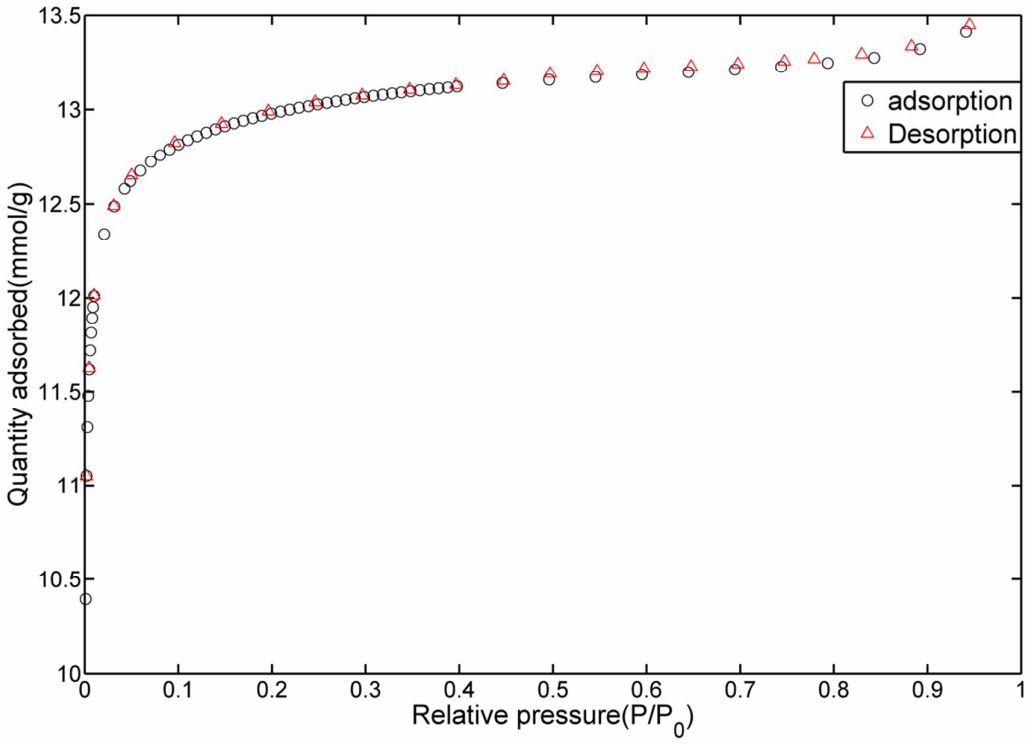


Figure S6: $N_2$ isotherm for MFM-300(Fe) at 77K.

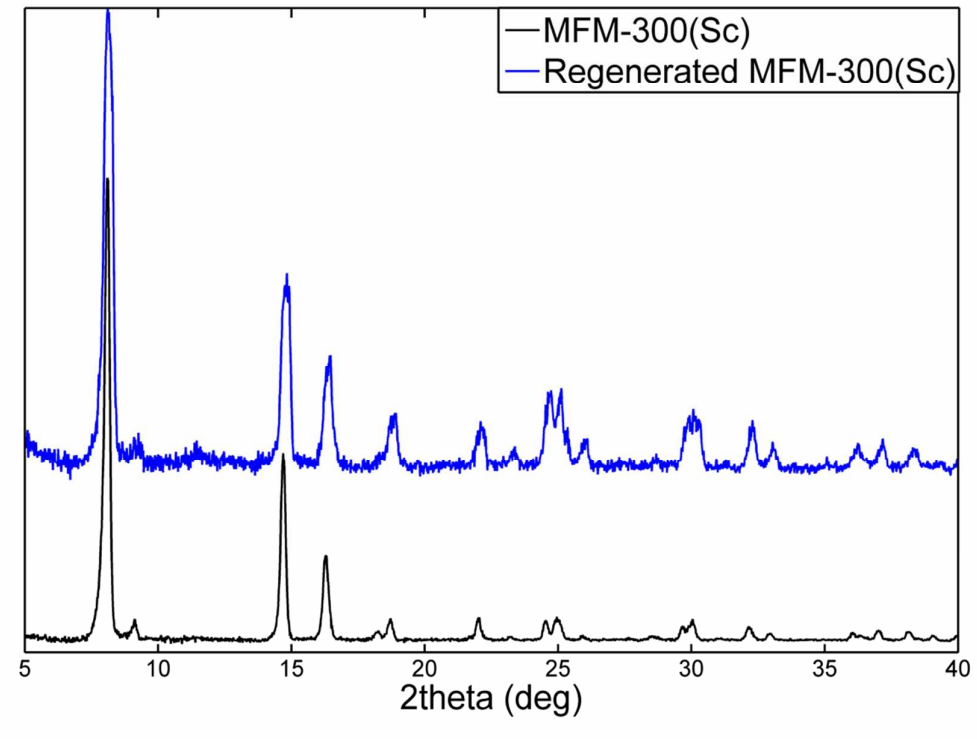


(a)

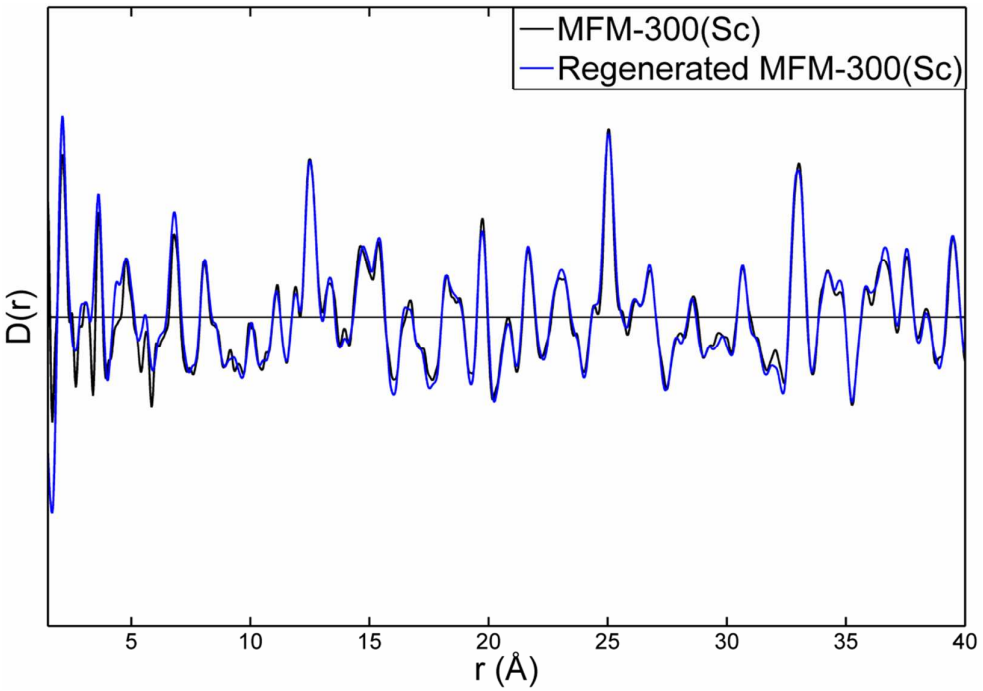


(b)

Figure S7: (a) Comparison of PXRD patterns for the bare MFM-300(Sc) and regenerated MFM-300(Sc) upon desorption of $I_2$. (b) Comparison of PDF data for the bare MFM-300(Sc) and regenerated MFM-300(Sc) upon desorption of $I_2$

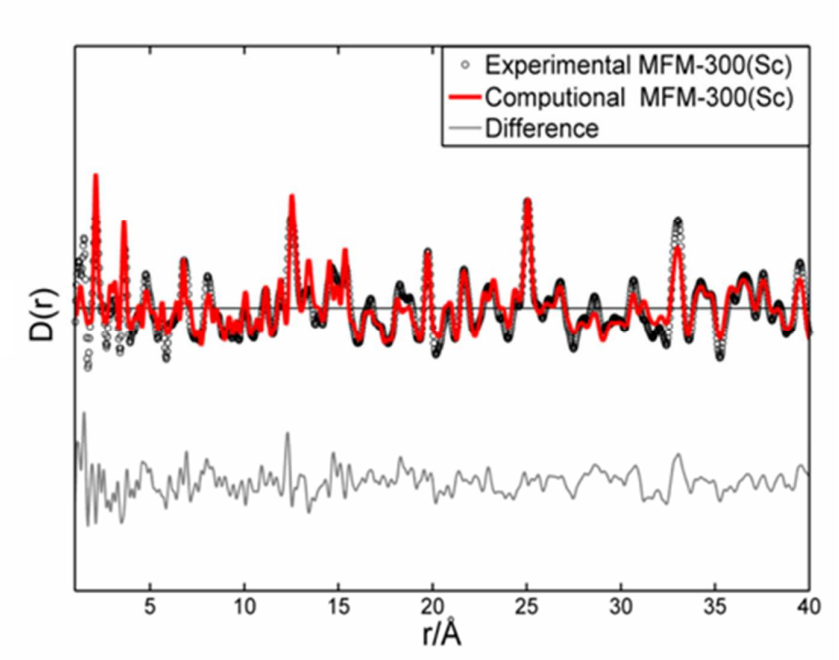


Figure S8: Comparison of the simulated and experimental PDF data for the bare MFM-300(Sc).

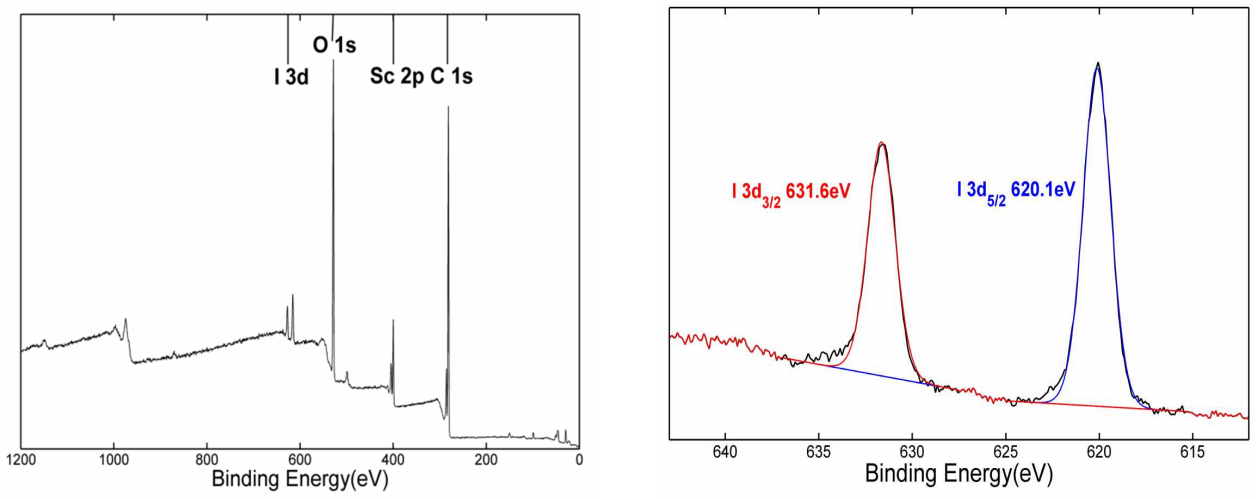


(a) (b)

Figure S9: XPS spectra of MFM-300(Sc)·2.62$I_2$. (a) full range (b) specific region for $I_2$.

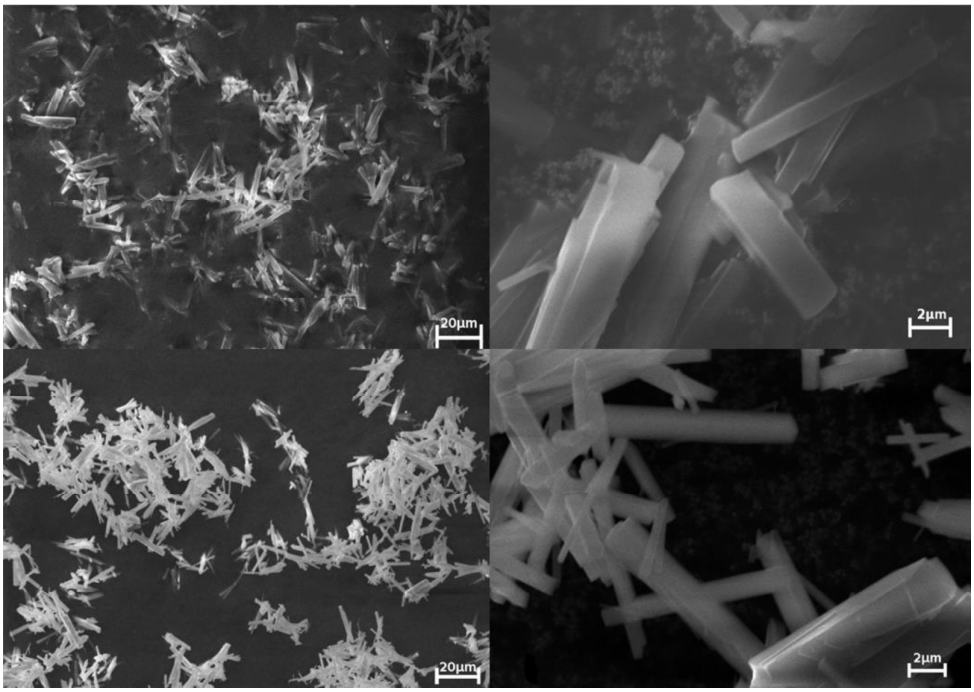


Figure S10: SEM images. top: MFM-300(Sc); bottom: MFM-300(Sc)·2.62$I_2$.

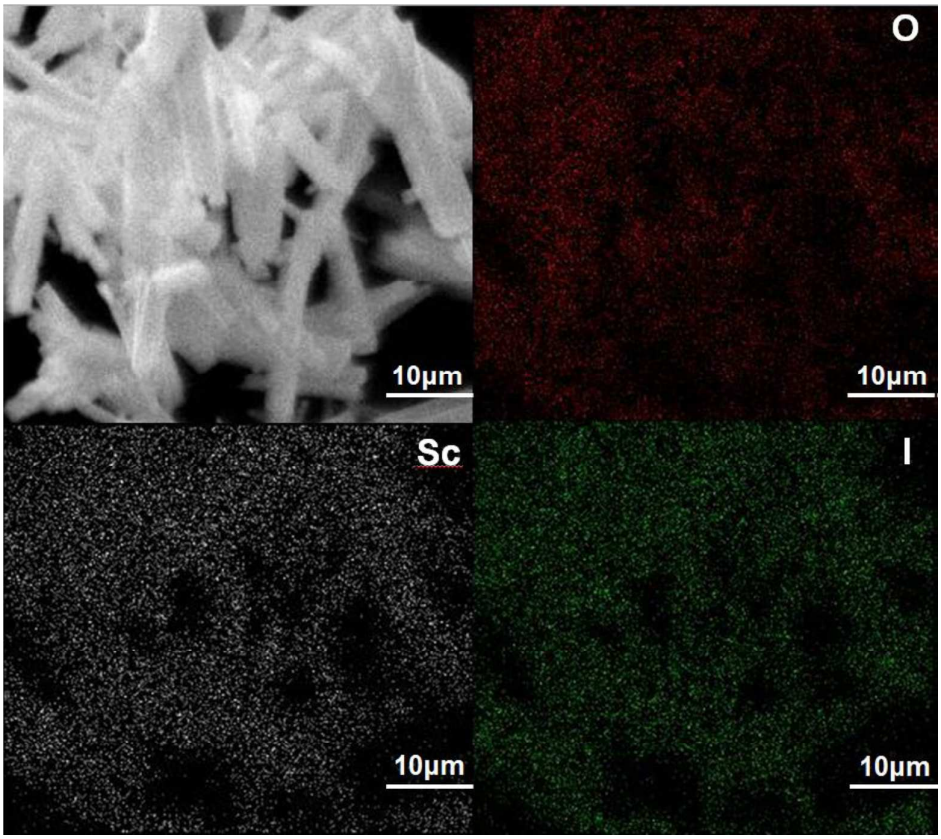


Figure S11: SEM-EDX images for MFM-300(Sc)·2.62$I_2$.

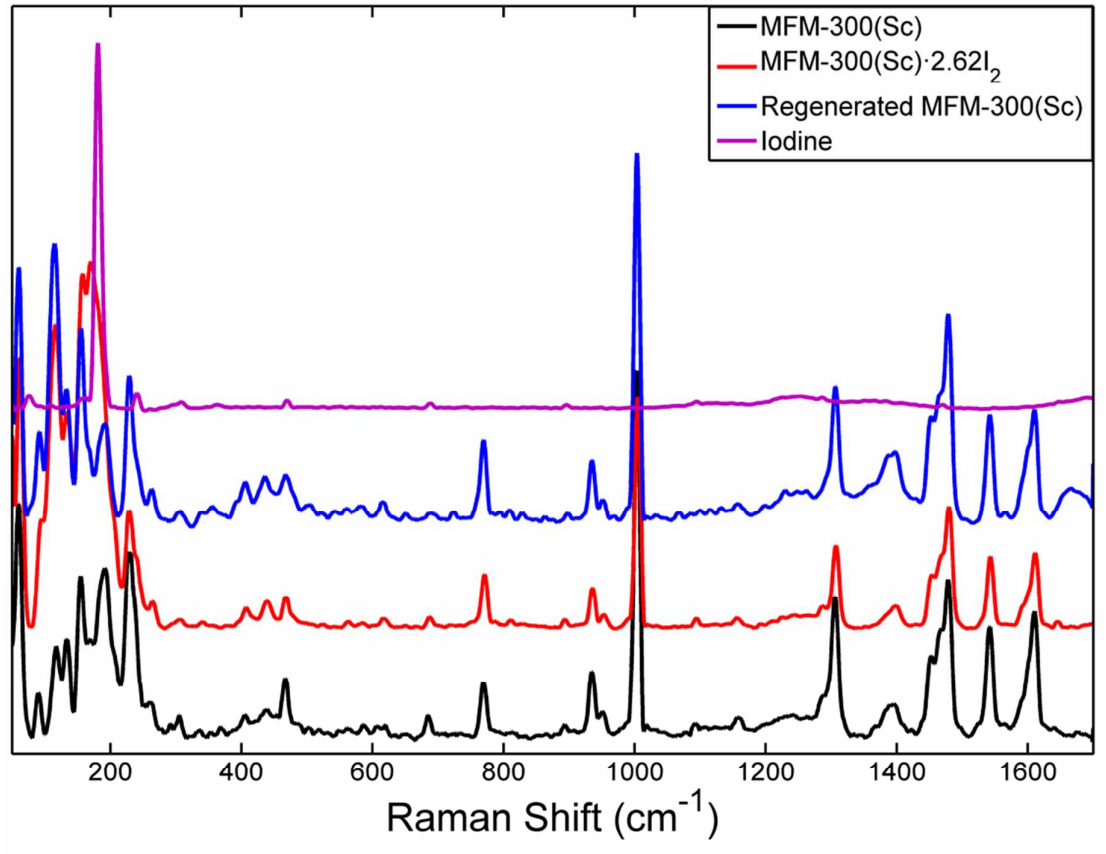


Figure S12: Raman spectra of MFM-300(Sc) as a function of $I_2$ loading.

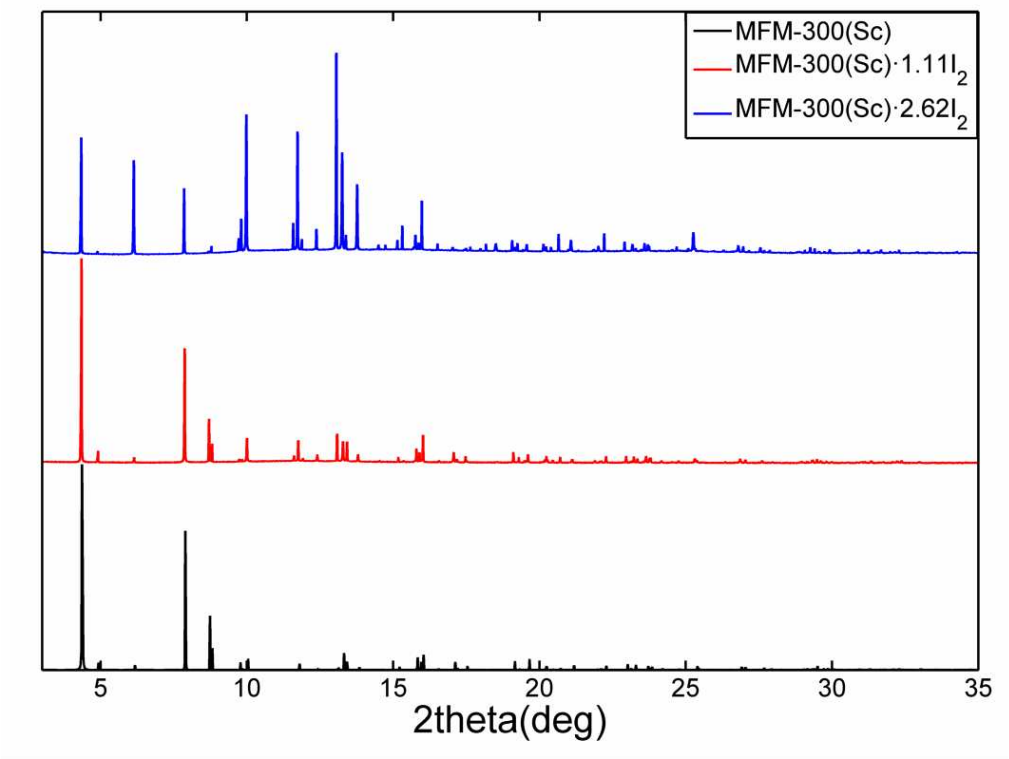


Figure S13: High resolution powder diffraction data for MFM-300(Sc) as a function of $I_2$ loading.

Table S1: Summary of powder X-ray diffraction refinements for MFM-300(Sc)·1.11$I_2$, MFM-300(Sc)·2.62$I_2$, desolvated MFM-300(Fe) and MFM-300(Fe)·1.11$I_2$.

| | MFM-300(Sc)·1.11$I_2$ | MFM-300(Sc)·2.62$I_2$ | MFM-300(Fe) | MFM-300(Fe)·1.11$I_2$ |
|---|---|---|---|---|
| Formula | $C_{16}H_8Sc_2O_{10}.I_{2.2168}$ | $C_{16}H_8Sc_2O_{10}.I_{5.232}$ | $C_{16}H_8Fe_2O_{10}$ | $C_{16}H_8Fe_2O_{10}.I_{2.2216}$ |
| Formula weight (g/mol) | 731.46 | 1114.08 | 471.92 | 753.84 |
| Temp / K | 298 | 298 | 298 | 298 |
| Radiation type | Synchrotron | Synchrotron | Synchrotron | Synchrotron |
| Diffractometer | Beamline I11 of Diamond Light Source | Beamline I11 of Diamond Light Source | Beamline I11 of Diamond Light Source | Beamline I11 of Diamond Light Source |
| Data collection mode | Transmission | Transmission | Transmission | Transmission |
| Wavelength (Å) | 0.827136(2) | 0.827136(2) | 0.827136(2) | 0.827136(2) |
| Crystal system | Tetragonal | Tetragonal | Tetragonal | Tetragonal |
| Space group | $I4_122$ | $I4_122$ | $I4_122$ | $I4_122$ |
| *a* / Å | 15.37392(3) | 15.40576(4) | 15.1061(2) | 15.11438(3) |
| *b* / Å | 15.37392(3) | 15.40576(4) | 15.1061(2) | 15.11438(3) |
| *c* / Å | 12.35373(3) | 12.39288(4) | 12.09237(14) | 12.03278(3) |
| V / $Å^3$ | 2919.897(14) | 2941.29(2) | 2759.41(8) | 2748.823(13) |
| $D_c$ /g $cm^{-3}$ | 1.664 | 2.518 | 1.136 | 1.822 |
| $R_{exp}$ / % | 3.86 | 3.44 | 4.66 | 3.66 |
| $R_{wp}$ / % | 6.81 | 6.12 | 8.98 | 6.76 |
| $R_p$ / % | 5.22 | 4.55 | 7.00 | 5.24 |
| *GoF* | 1.77 | 1.78 | 1.93 | 1.85 |
| $R_{Bragg}$ | 3.73 | 3.79 | 3.34 | 2.40 |
| CCDC deposition number | 1558479 | 1558480 | 1558481 | 1558482 |

**Additional views for MFM-300(Sc)·1.11$I_2$ and MFM-300(Sc)·2.62$I_2$**

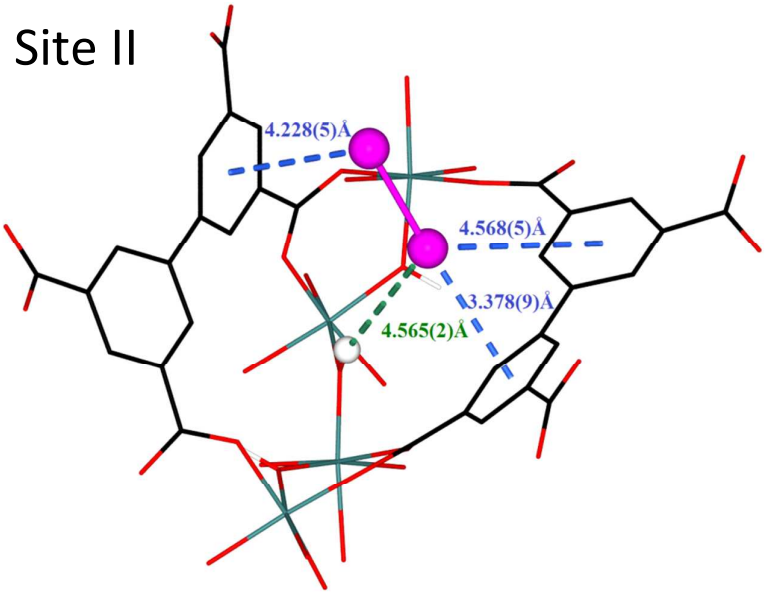


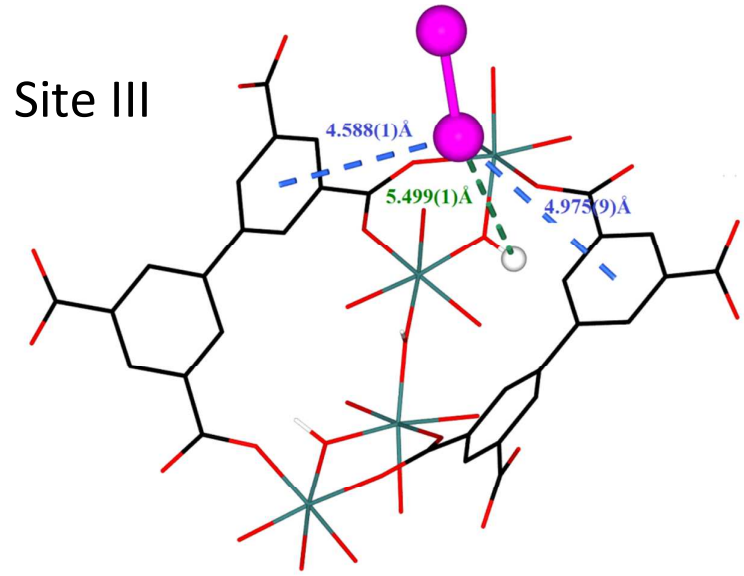

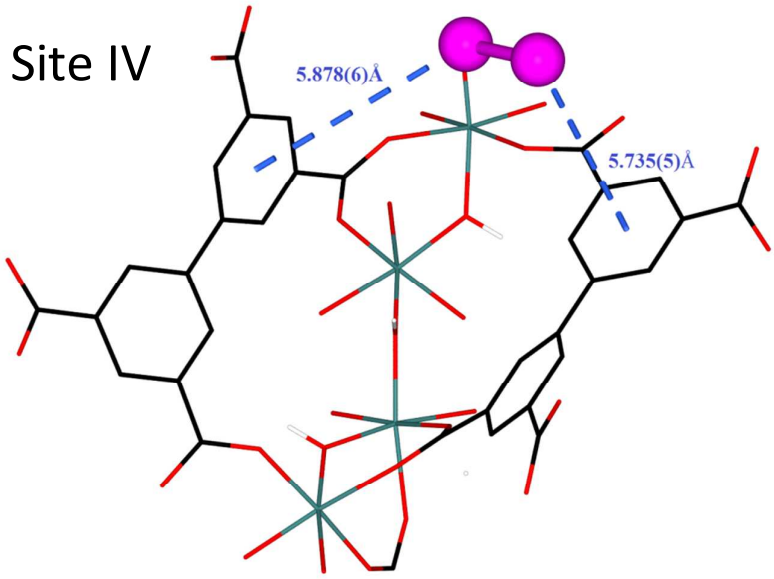


Figure S14: Views of different $I_2$ binding sites for MFM-300(Sc)·1.11$I_2$.

Site II’

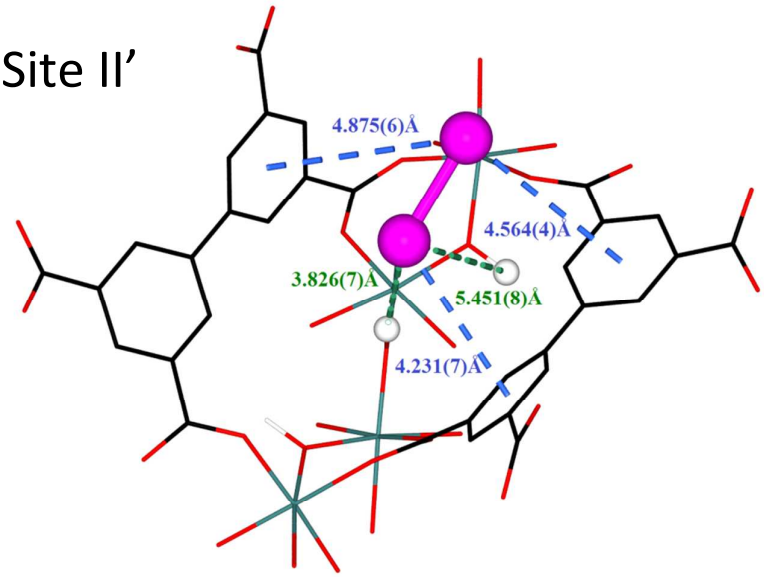


Site III’

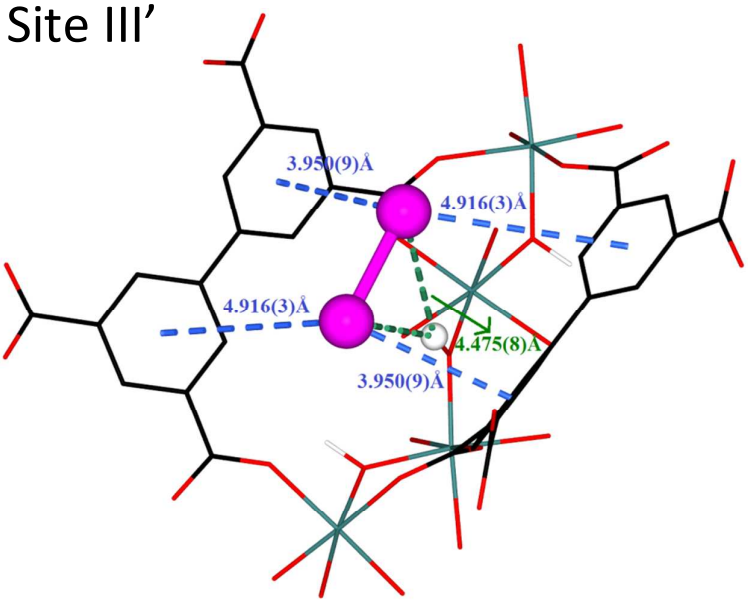

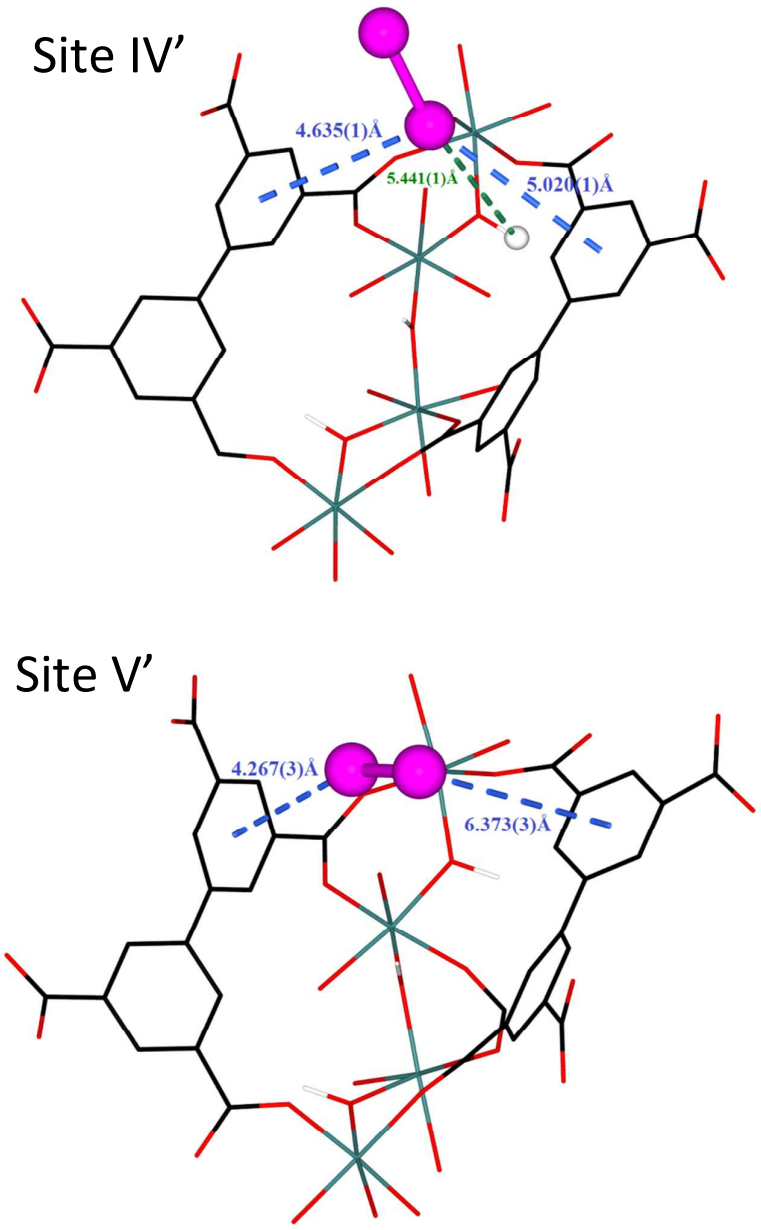


Figure S15: Views of different $I_2$ binding sites for MFM-300(Sc)·2.62$I_2$.

**Additional views for MFM-300(Fe)·1.11$I_2$**

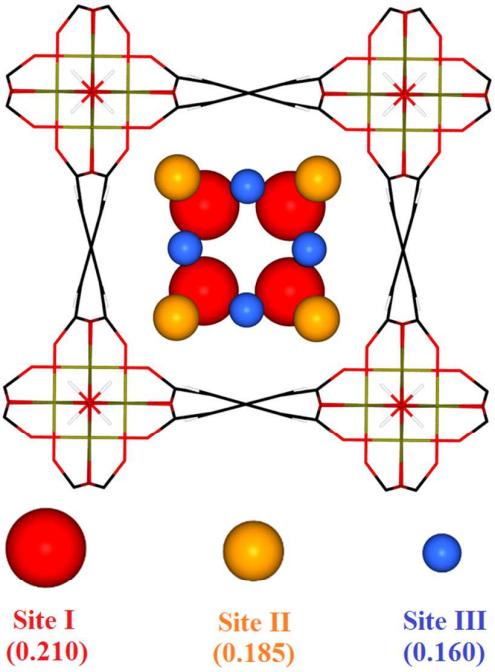


Figure S16: Views along *c* axis of the binding sites and occupancies for adsorbed $I_2$ molecules in MFM-300(Fe)·1.11$I_2$.

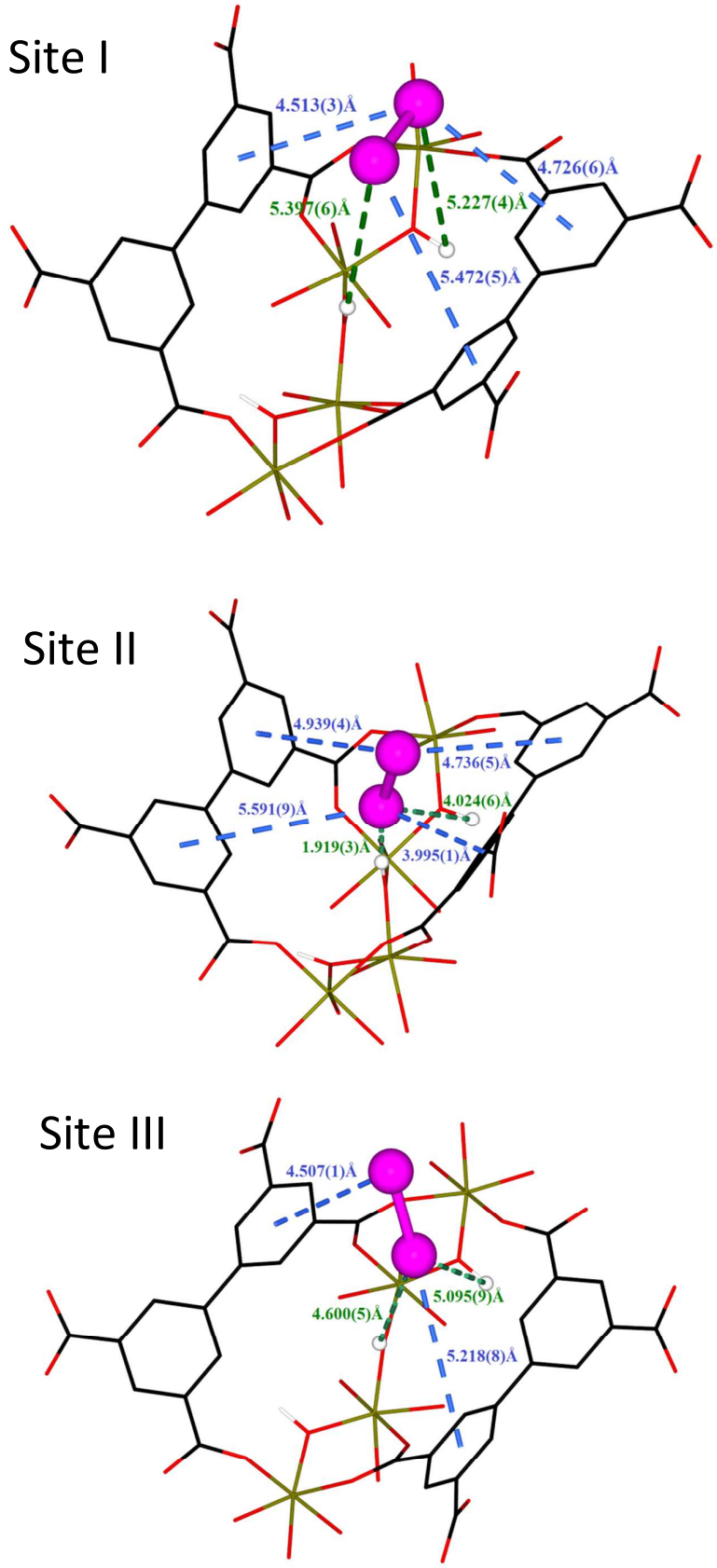


Figure S17: $I_2$ binding sites for MFM-300(Fe)·1.11$I_2$.

Table S2: Crystal data and structure refinement for MFM-300(In)·0.5$I_2$.

| Complex | MFM-300(In)·0.5$I_2$ |
|---|---|
| Empirical Formula | $C_{16}H_8I\ In_2O_{10}$ |
| Molar mass, g $mol^{-1}$ | 716.76 |
| Temperature, K | 120(2) |
| Crystal system | Tetragonal |
| Space group | $I4_122$ |
| *a*, Å | 15.4373(2) |
| *b*, Å | 15.4373(2) |
| *c*, Å | 12.3120(2) |
| *V*, / $Å^3$ | 2934.08(9) |
| *Z* | 4 |
| $D_{calcd}$, g $cm^{-3}$ | 1.623 |
| F(000) | 1340 |
| μ, $mm^{-1}$ | 2.66 |
| Crystal size, mm | 0.060 × 0.020 × 0.005 |
| θ range, deg | 2.558 – 24.977 |
| Limiting indicies *hkl* | $-18 \le h \le 16, -17 \le k \le 17, -14 \le l \le 14$ |
| Reflections collected / independent | 6405 / 1247 |
| $R_{int}$ | 0.0906 |
| Reflections with $I > 2\sigma(I)$ | 996 |
| Goodness-of-fit on $F^2$ | 1.129 |
| Final *R* indices [$I > 2\sigma(I)$] | $R_1 = 0.0956$, $wR_2 = 0.2780$ |
| *R*-indices (all data) | $R_1 = 0.1122$, $wR_2 = 0.2657$ |
| Largest difference in peak and hole, *e*/$Å^3$ | 2.634 / –1.061 |
| CCDC deposition number | 1558478 |

Table S3. Selected bond length (Å) for MFM-300(In)·0.5$I_2$

| Bond | *d*, Å |
|---|---|
| In1—O1M | 2.103 (18) |
| In1—O1M$^{i}$ | 2.103 (18) |
| In1—O12$^{ii}$ | 2.104 (14) |
| In1—O12$^{iii}$ | 2.104 (14) |
| In1—O11 | 2.162 (15) |
| In1—O11$^{iv}$ | 2.162 (15) |
| I1—I1$^{v}$ | 2.64 (6) |
| I2—I2$^{vi}$ | 2.49 (5) |

Symmetry transformations used to generate equivalent atoms: (i) *y*+1/2, –*x*+1, *z*–1/4; (ii) –*x*+3/2, *y*, –*z*+3/4; (iii) –*y*+1, *x*–1/2, *z*+1/4; (iv) –*y*+1, –*x*+1, –*z*+1; (v) *x*, –*y*+1/2, –*z*+5/4; (vi) *y*, *x*, –*z*+1.

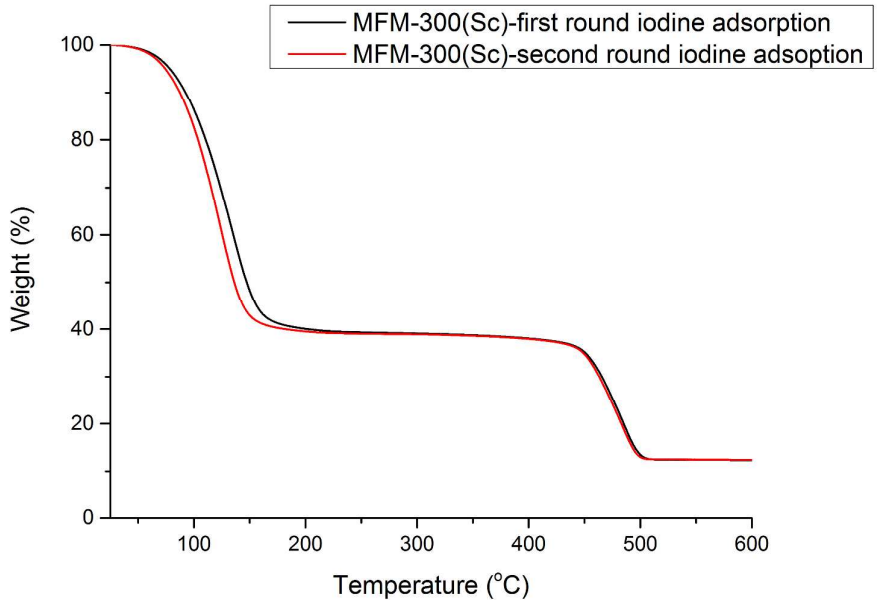


Figure S18. TGA plots and $I_2$ adsorption capacities of MFM-300(Sc) for adsorption-desorption cycling tests.